INDONESIAN JOURNAL OF SOCIAL AND ENVIRONMENTAL ISSUES (IJSEI)
Journal Homepage: https://ojs.literacyinstitute.org/index.php/ijsei
ISSN: 2722-1369 (Online)
Research Article

Volume 4	Issue 3	December (2023)	DOI: 10.47540/ijsei.v4i3.1218	Page: 353 – 375

Hydrological Impacts of Climate Change (Rainfall and Temperature) and Characterization of Future Drought in the Aga Foua Djilas Watershed

Philippe Malick Dione[1], Cheikh Faye[1], Cheikh Abdoul Aziz Sy Sadio[1]
[1]Department of Geography, U.F.R. Sciences et Technologies, Assane Seck University of Ziguinchor, Laboratoire de Géomatique et d'Environnement, BP 523 Ziguinchor, Senegal
Corresponding Author: Philippe Malick Dione; Email: pm.d11@zig.univ.sn

A R T I C L E I N F O

Keywords: Climate Change; Drought; Hydrological Impacts; Watershed.

Received : 19 November 2023
Revised : 20 December 2023
Accepted : 28 December 2023

A B S T R A C T

Studying climate change's impact on runoff and drought is crucial for sustainable society and ecosystems. The extent of drought evolution and how droughts would affect society and the environment are not sufficiently considered in Senegal. This study assesses hydrological impacts and future drought using three global climate models (ACCESS-ESM1-5, BCC-CSM2-MR, and MRI-ESM2-0) as part of the Coupled Model Intercomparison Project (CMIP6) in the Aga-Foua-Djilas Basin. To this end, the hydrological impacts of climate change over 20-year periods (2021-2040; 2041-2060; 2061-2080; 2081-2100) at a resolution of 2.5 under four emission scenarios (SSP 126; 245; 370; 585), were investigated, and the drought characteristics are shown below, the SSP 245 and 585 scenarios over the 2021-2100 period. The results highlight a decrease in runoff potential given the drop in rainfall, which fell from 25.2 mm over the 2021-2040 period and under SSP 126 to 2.4 mm towards the end of the century (2081-2100) and under the SSP 585 scenario, changes in the standardized precipitation index (SPI) and the standardized precipitation and evapotranspiration index (SPEI) were first compared, and the SPEI showed larger changes due to its inclusion of temperature effects. The drought zone in the basin is likely to increase at the end of the 21st century with values approaching 80% for SPI and 90% for SPEI under the SSP 245 and SSP 585 scenarios if drought mitigation and adaptation mechanisms are inadequate. The results provide important guidance for improving the identification of causes, minimizing impacts, and building resilience to droughts in Senegal.

INTRODUCTION

Climate change impacts human ecosystems, societies, and economies in diverse ways; water is the main intermediary through which we feel its impacts. In some cases, these consequences are obvious, such as increased frequency and intensity of storms, floods, and droughts. Increased variability in the global water cycle leads to greater water stress at different times and in different regions (Milly et al., 2005). Water-related impacts of climate change also include adverse effects on food security, human health, energy production, and biodiversity, not to mention the daily livelihoods of women, men, and children. the most vulnerable. These effects can lead (or have already led) to growing social inequalities, social unrest, mass migrations, and conflicts. Climate change and accelerating population growth have become major factors limiting the sustainable development of human resources and the conservation of natural systems. Rainfall is a fundamental climatic factor, the importance of which translates well into groundwater recharge, the availability of water resources, and consequently the socio-economic benefits, including the agricultural yields that depend on it (Sultan and Janicot, 2006).

One of the major challenges of research on climate variability, particularly rainfall, is to quantify its impact on water resources and the natural environment. The waters of the lowlands, used for agricultural production, mainly come from rain and groundwater which is flush with it, water used for agricultural production. However, some rice-growing plots in the neighborhoods adjoining the Casamance River are gradually being salinized, following the advance of the salt bevel. Under these conditions and in view of the importance of the sectors of activity (rice growing, market gardening, etc.) affected, the populations become impoverished and become more vulnerable to climatic risks (Mbaye et al., 2011).

Furthermore, in a single environmental sector, the impacts of climate change are determined by a certain number of climatic variables. For example, runoff generation in a watershed is typically determined by precipitation, temperature, and other climatic variables. However, in impact studies, it is difficult to determine the relative importance of each climate variable. To address this, previous studies have generally indicated that all variables are equally important and given equal weight (Xu et al., 2010; Chen et al., 2017; Zhao, 2015). However, these climatic variables generally do not have the same importance in the field of impact. For example, precipitation may be more important than temperature for a precipitation-dominated watershed, but it could be different for a snowfall-dominated watershed.

Thus, it may be simpler to calculate GCM weights based on their ability to replicate the single impact variable instead of multiple climate variables. Such a method would integrate the synthetic capacity of GCMs in terms of simulating several climatic variables with that of an impact variable. Moreover, this method could also circumvent the previous problem of potential non-linearity between the climatic variables and the impact variable. In this context of climate change, and to manage the water resources of the Aga- Foua - Djilas basin in a reasoned way, it is necessary to have as clear an idea as possible of how the catchment area will respond to changes. climate (Kouassi et al., 2017). The question raised by this study is therefore the following: What will be the hydrological impacts of climate change in the Aga-Foua - Djilas watershed?

In its Sixth Assessment Report, Working Group I of the Intergovernmental Panel on Climate Change (IPCC) concludes: There is no doubt that human activity has caused global warming of the atmosphere, oceans, and soils. He also believes that "the scale of the recent upheavals experienced by the climate system as a whole and the current state of this system in many respects are unprecedented for several centuries, even several millennia" (IPCC, 2021).

There are many reasons to believe that these physical climate changes will have different types of socio-economic impacts – with associated losses and damages – including direct impacts on people's livelihoods. These could manifest themselves, for example, in changes in precipitation patterns, temperatures, and the distribution of biodiversity and ecosystem services. Another indirect effect on livelihoods includes changing the demand for goods and services (Granderson, 2014).

Unlike many natural risks, which occur suddenly and locally – floods, earthquakes, landslides, etc. – a drought is a phenomenon with slow dynamics and wide spatial extension. Its gradual installation makes it a so-called "cumulative" risk where damage occurs when thresholds are crossed (Leone et al., 2010). As confirmed by the latest IPCC report (IPCC, 2021), the influence of climate change under a regime of global temperature rise is not trivial concerning the risk of drought. Drought may not be considered a pure "natural hazard", as humans have altered the characteristics of drought (Tang, 2020). As global warming increases, the magnitude of climate change impacts on the environment and society increases (Touma et al., 2015; Ault et al., 2016; Leng et al., 2015).

An increase in food demand due to rapid population growth can lead to severe food insecurity and challenge the United Nations (UN) 2030 zero hunger agenda, which should be achieved by ensuring sustainable development (FAO, 2017; Fujimori et al., 2019). In addition, rapid population growth has increased water consumption, which has dramatically intensified the frequency of global droughts by 27% (Wada et al., 2013). Even if it is difficult to precisely quantify the evolution of the frequency and intensity of droughts in our latitudes due to the absence of climatological data series of sufficient quality, the combination of these factors will favor the appearance of droughts by generating greater evapotranspiration, accentuating the risk of drying out of soils and freshwater reserves.

In a context of climate change where the quantity and quality of the planet's freshwater resources are increasingly under pressure from demographic growth and economic activity, West Africa seems to be facing these decades to prolonged and severe droughts, particularly in its semi-arid Sahelian region and without forgetting the serious and devastating floods recorded in its humid tropical zone (Janicot et al., 2015). As a result, most river basins in this part of the globe are faced with these same hydroclimatic events. To study the impact of climate change on hydrology, several global climate models (GCMs) and several emissions scenarios have been widely used to drive hydrological models (IPCC, 2013; Chen et al., 2011). Designed through different assumptions and unique mathematical representations of the physical processes of the climate system, GCMs offer different climate projections (Konapala et al., 2020; Laurent et al., 2020). The Intergovernmental Panel on Climate Change (IPCC) provides regularly (approximately every 7 years) an inventory of scientific knowledge on climate change, in the 21st century and beyond, in its evaluation reports. The 6th report (IPCC, 2021) therefore offers new estimates, based on the latest generation of climate models, on a global scale and the scale of large regions Konapala et al., 2020; Laurent et al., 2020).

According to different sources, it is climatic variations, affecting the hydrological cycle, which increases the frequency and severity of droughts in several regions of the world (Nguvava et al., 2019; Osima et al., 2018; Spinoni et al., 2020). Thus it is very important to assess the extent of projected droughts and their impacts in West Africa and how its impacts would affect society and the environment, these elements remaining largely unexplored. This was initiated to bridge through the understanding of future drought severity levels (moderate, severe, and extreme) and characteristics (event, duration, frequency, and intensity) at different spatiotemporal scales. In a context where dry regions tend to become drier and humid regions tend to become wetter (Feng & Zhang, 2015; Moraes Frasson et al., 2019; Yang et al., 2019), the study of impacts of climate change on drought remains fundamental. In a Senegalese context, studying the phenomenon of droughts and the projected impact of climate change on future drought conditions would be of great importance to society and policymakers. This could help in effective drought mitigation, adaptation, and reduction of future drought risks. This article therefore aims to characterize the hydrological impacts of climate change and to analyze the drought time series and the main changes in drought characteristics in the Aga-Foua-Djilas basin.

MATERIALS AND METHODS

Study area

Aga-Foua-Djilas watershed is located in the northern and northwestern part of the Sine Saloum delta. The latter is one of the major hydrological basins that drain Senegal. It is drained by a network of rias, the two main ones bearing the names of Sine and Saloum. The basin is crisscrossed by many small lowlands which, despite the persistent drought, each winter drains large quantities of runoff water. In latitudes, it extends between 14°15'N and 14°25'N and in longitudes, between 16°37'W and 16°53'W. It covers an area of 317.5 km2, with a perimeter of 115.7 km. Administratively, it straddles the Communes of Malicounda, Sandiara, Séssène and Nguéniène (Department of Mbour), Tattaguine, Loul Séssène and Djilas (Department of Fatick).

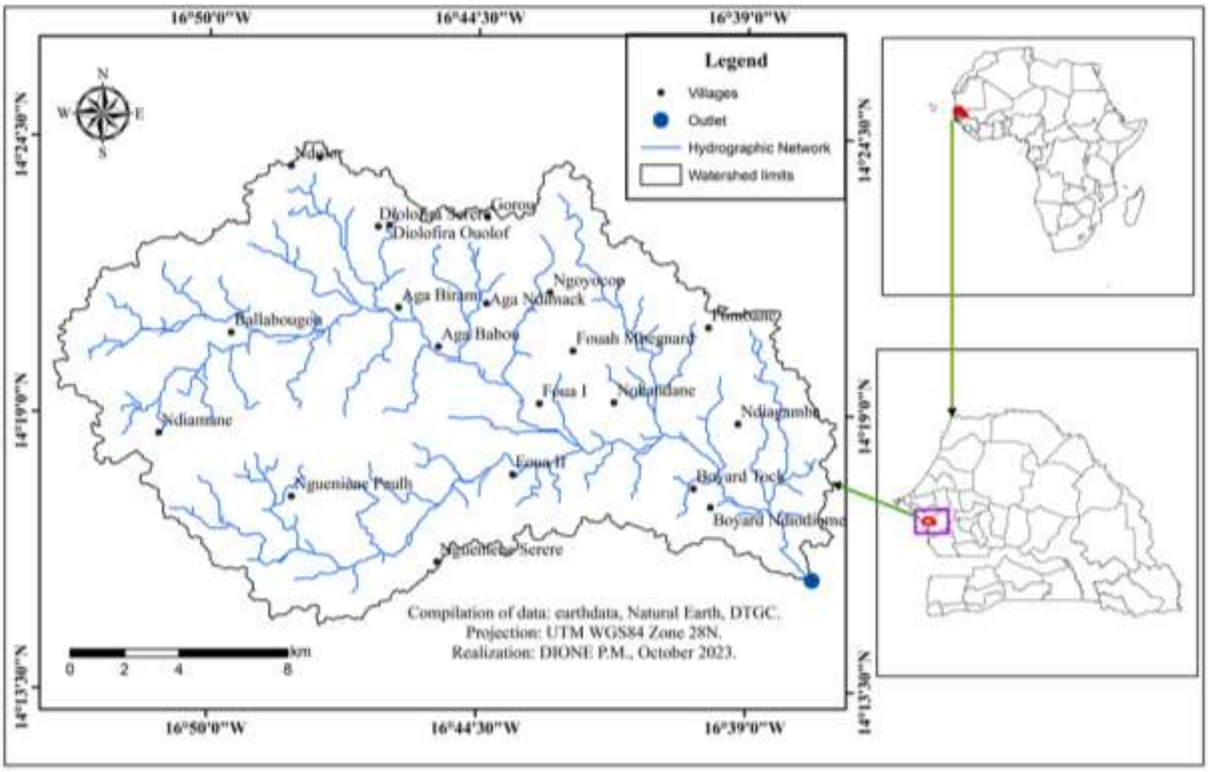

Figure 1. Presentation of the Aga- Foua - Djilas Basin

Data

To determine the impact of climate change on future rainfall and temperatures in the Aga-Foua-Djilas basin, four climate change scenarios are used, the SSPs. These describe alternative futures of socio-economic development and represent, based on narrative and quantitative variables, how the world might change in the coming decades and what challenges these changes pose for mitigation and adaptation. The data used come from five models (tMRI-ESM2-0, CNRM-CM6-1 f2, CNRM-CM6-1-HR f2, GFDL-ESM4, and CESM2-WACCM) selected from about twenty models and which generate a better representation of the climate in terms of mean state and variability. The scenarios were downloaded from the interface https://climexp.knmi.nl/selectfield_cmip6.cgi?id=someone@somewhere accessed on July 01, 2023). The data extracted from the five models retained in this study are the precipitation and maximum, average, and minimum temperature data for the future period (2021-2100). For future projections, we have defined four characteristic periods for each scenario: the near future ranging from 2021 to 2040 (horizons 2040 or beginning of the 21st century); the average future 1, from 2041 to 2060 (horizon 2060 or mid-21st century); the average future 2, from 2061 to 2080 (horizon 2080); the distant future varies from 2081 to 2100 (horizon 2100 or end of the 21st century). For the data used in the characterization of the drought, they come from this multi-modal set and two scenarios (SSP 245 and SSP 585) over the period 2021-2100.

Determination of Hydrological Parameters

The hydrological parameters evaluated in this paper are effective rainfall, runoff potential, and infiltration potential.

Efficient Rain Determination

At the scale of a watershed, the evaluation of water resources requires the most precise knowledge possible of the various terms of the hydrological balance, in particular effective rainfall. Indeed, for hydrologists and hydrogeologists, effective rainfall corresponds, in its broadest sense, to the “part of the rain that contributes to runoff” (Vittecoq et al., 2010).

In the broad sense, we call “effective rain (Pe)”, the rain-giving rise to a flow, superficial or underground, immediate or deferred. This term of the water balance conditions the availability of water, whether in terms of its rapid surface transfer (runoff) or its delayed flow through aquifers (Kouassi et al., 2017). The effective rainfall can be expressed by the following relationship (Equation 1):

$$P_e = P - ETR \text{ .... } (1)$$

With P_e: effective rain (mm); P: rainfall (mm); ETo: actual evapotranspiration (mm).

Determination of Actual Evapotranspiration (ETo)

The ETo was determined using the Coutagne method. This method gives good results in the study of water balance (Kouassi et al., 2012). The actual evapotranspiration (ETo) is given by the following expression (Equation 2):

$$ETR = P - \gamma P^2 \text{ .... } (2)$$

Where: $\gamma = 1/(0{,}8 + 0{,}145t)$

With t being the average annual temperature in °C and P the average annual precipitation in m. This method is only applicable if *1/8 < P < 1/2* with P in m.

Determination of PET

The potential evapotranspiration (PET) is calculated by the method of Thornthwaite (Kouassi et al., 2012; Don't Guessan et al., 2014) whose formula is as follows:

$$ETP\ (\text{mm mois}) = 16\left(\frac{10t}{I}\right)^a \times F(\gamma)$$

Where *t* is the monthly mean temperature in °C, and I is the annual heat index. It is the sum of the twelve-monthly thermal indices *i (m)* and is given by the following formula:

$$I = \sum_{m=1}^{12} i\ (m) \text{ .... } (5)$$

With *i (m)*, the monthly thermal index which is presented as follows:

$$i(m) = \left(\frac{t}{5}\right)^{1{,}514} \text{ .... } (6)$$

The variable *a* is a complex function of the thermal index *I* with:

$$a = 0{,}\ 49239 + 1{,}\ 79.10^{-2}\ I - 7{,}\ 71.10^{-5}\ I^2 + 6{,}\ 75.10^{-7}\ I^3 \text{ .... } (7)$$

$F(\gamma)$, the corrective factor is a function of the latitude of the place considered and of the given month. Its values are tabulated.

Determination of Runoff Potential (R)

Tixéront-Berkaloff formula which uses the rainfall and the PET calculated by the method of Thornthwaite (Kouassi et al., 2012; Don't guessan et al., 2014). The Tixéront-Berkaloff formula for the evaluation of runoff (R) is as follows:

$$R = \frac{P^3}{3ETP^2} \text{ .... } (8)$$

Where R is the runoff in mm; P the average annual precipitation in mm; PET the average annual potential evapotranspiration calculated by the Thornthwaite method in mm.

Determination of Infiltration Potential (I)

The hydrological balance method is the most widely used for determining the amount of infiltrated water (Kouassi et al., 2012; N'guessan et al., 2014). Infiltration is evaluated from the following equation:

$$I = P - (ETo + R) + \Delta S \text{ .... } (9)$$

With: I: the infiltrated water depth (mm); P: rainfall (mm); ETo: actual evapotranspiration (mm); R: the layer of runoff water (mm); ΔS: the variation of the water stock.

The work was carried out based on the assumption that, at the scale of the annual hydrological cycle, stock variations cancel each other out over a large basin (Mahé et al., 2005).

SPI Analysis

The SPI analysis was performed based on historical rainfall data for the period 1985-2014, and on two SSPs for the period 2021-2100: (i) SSP 245, a medium adaptation challenge scenario that describes a world characterized by the pursuit of current trends, very close to the "Inertia" family; and (ii) SSP 585, a very high baseline emissions scenario that describes a world that focuses on the traditional and rapid development of developing countries based on high energy consumption and carbon-emitting technologies. The SPI was calculated using the ClimPACT program. This program is based on the RClimDEX program, which was created by the WMO Expert Team on Climate Change Detection and Indices (Shiferaw et al., 2018).

SPI is a probability index derived solely from precipitation statistics for a certain location and period (months or years). This index converts the cumulative probability into the standard normal random variable (Van Vuuren et al., 2011). The median precipitation value and the SPI quantify the probability of observing a given amount of precipitation in a certain time (Saada et al., 2017). Negative and positive SPI values indicate dry and wet conditions respectively; these values become more negative or positive, respectively, as dryness or humidity increases (Butu et al., 2020). In this study, three-month (SPI 3) (January-March), six-month (SPI 6) (January-June), and twelve-month (SPI 12) (January-December) SPIs were used to describe, respectively, seasonal changes in precipitation, changes corresponding to agricultural drought, annual changes and longer-term trends corresponding to hydrological drought (Zeybekoglu et al., 2021).

The dataset has evolved, and a new SPI value is added every month, derived from the calculated values of previous months. The probability of any observed precipitation data point was calculated from historical records. This probability was used in conjunction with an estimate of the inverse normal to calculate the deviation of precipitation from a normally distributed probability density with mean zero and standard deviation of unity. This number was the SPI for the precipitation data point (Javanmard et al., 2017).

Given a normal distribution function with zero mean and variance, the SPI was calculated as (Fung et al., 2019):

For $0 < H(x) \leq 0.5$,

$$SPI=-\left(t-\frac{c_0+c_1+c_2+t^2}{1+d_1t+d_2t+d_3t}\right), \quad t=\sqrt{\ln\frac{1}{(H(x))^2}} \quad \text{.......... (10)}$$

For $0.5 < H(x) \leq 1$,

$$SPI=+\left(t-\frac{c_0+c_1+c_2+t^2}{1+d_1t+d_2t+d_3t}\right), \quad t=\sqrt{\ln\frac{1}{(1{,}0-H(x))^2}} \quad \text{.......... (11)}$$

where c_0= 2.515517, c_1= 0.802853, c_2= 0.010328, d_1= 1.432788, d_2= 0.189269 and d_3= 0.001308 (Javanmard et al., 2017).

SPI results were categorized as Extremely Dry to Extremely Wet, as proposed by McKee et al. (1993), as shown in Table 1.

Table 1. Classification of Drought Sequences According to SPIs

SPI values	Sequences of droughts	SPI values	Wet footage
-1.00< SPI <0.00	slightly dry	0.00< SPI <1.00	slightly damp
-1.50< SPI <-1.00	Moderately dry	1.00< SPI <1.50	Moderately humid
-2.00< SPI <-1.50	Severely dry	1.50<SPI<2.00	Severely wet
SPI < -2.00	extremely dry	2.00< SPI	Extremely wet

SPEI Calculation Methods

In this study, SPEI was used to monitor and quantify future drought in the SFM basin. The analysis is made based on historical precipitation data for the period 1985-2014, and on two SSPs (245 and 585) for the period 2021-2100. The SPEI is considered an improved drought index, particularly suitable for analyzing the effect of global warming on drought conditions (Beguería et al., 2015). The calculation of the SPEI in this study follows the method mentioned in the study by Vicente-Serrano et al. (2010). The SPEI is based on a climatic water balance which is determined by the difference between Precipitation (P) and potential evapotranspiration (PET) for month i:

$$D_i = P_i - ETP_i \quad \text{.......... (12)}$$

D_i provides a simple measure of water surplus or deficit for the analyzed month. The PET is calculated according to the Thornthwaite equation (Thornthwaite, 1948).

The calculated values D_i are aggregated at different time scales, following the same procedure as for the SPI. The difference $D_{i,j}^k$ in a given month j and year i depends on the chosen time scale, k. For example, the difference accumulated during a month of a given year, with a time scale of 12 months, is calculated according to the following formula:

$$X_{i,j}^{k}= \sum_{I=13-k+j}^{12} D_{i-I,j}+\sum_{I=1}^{j} D_{i,j} \text{, si } j<k \text{, et} \quad \ldots \quad (13)$$

$$X_{i,j}^{k}= \sum_{I=j-k+j}^{j} D_{i,j} \text{, si } j\geq k \quad \ldots \quad (14)$$

Where $D_{i,j}$ is the difference in P-PET of the *lth* month of year i, in mm.

And then the log-logistic distribution is selected to normalize the D-series to obtain the SPEI. The probability density function of the log-logistic distributed variable is expressed as follows:

$$f(x)= \frac{\beta}{\alpha}\left(\frac{x-\gamma}{\alpha}\right)^{\beta-1}\left[1+\left(\frac{x-\gamma}{\alpha}\right)^{\beta}\right]^{-2} \quad \ldots \quad (15)$$

Where α, β, and γ are the scale, shape, and origin parameters, respectively, for D values in the range ($\gamma > D < \infty$). Thus, the probability distribution function of series D is given by:

$$F(x)= \left[1+\left(\frac{\alpha}{x-\gamma}\right)^{\beta}\right]^{-1} \quad \ldots \quad (16)$$

With F(x), the SPEI can easily be obtained as normalized values of F(x). For example, following the classical approximation of Abramowitz and Stegun (1965):

$$SPEI=W- \frac{C_0+C_1W+C_2W^2}{1+d_1W+d_2W^2+d_3W^3} = \quad \ldots \quad (17)$$

Where $W=\sqrt{-2\ln(p)}$ for $p\leq 0.5$ and p is the probability of exceeding a determined D value, p = 1 - F (x). If p > 0.5, p is replaced by 1 - p and the sign of the resulting SPEI is reversed. The constants are: C_0 = 2.515517, C1 = 0.802853, C_2 = 0.010328, d_1 = 1.432788, d_2 = 0.189269 and d_3 = 0.001308. Positive SPEI values indicate above-average wet conditions, while negative values indicate dry conditions. A drought event is defined when the value of SPEI is less than or equal to -1 during a certain period. The drought categories based on SPEI values are analogous to that in Table 1 proposed by McKee et al. (1993) for SPIs.

Methodology for Analyzing the Hydrological Impacts of Climate Variability

Pettitt test (1979)

A break is defined as a change in the law of probability of the random variables whose successive realizations define the time series studied (Servat et al., 1998). Pettitt 's test was chosen for its power and robustness (Lubès -Niel et al., 1998). Pettitt 's test is a non-parametric test for detecting a single rupture with an unknown date. Pettitt 's variable $(U_{t,N})$ is defined by equation 18.

$$U_{t,N}=\sum_{i=1}^{t}\sum_{j=t+1}^{N} D_{ij} \quad \ldots \quad (18)$$

With:

$$S= \sum_{i=1}^{k}\sum_{j=k+1}^{n} \text{signe}\,(x_j-x_i) \quad \ldots \quad (19)$$

If the null hypothesis is rejected, an estimate of the break date is given by the instant t defining the maximum in the absolute value of the variable U t, N (Soro et al., 2011). It can be noted that the test also provides an estimate of the position of the break using the index k corresponding to the maximum U (k)|.

The hydrological deficit with respect to the ruptures identified by the Pettitt test was evaluated from equation 12 (Ardoin, 2004):

$$D=\frac{X_j}{X_i}-1 \quad \ldots \quad (20)$$

Or Xj is the mean of the series after the break and $\overline{(Xi)}$ the one before the break.

Mann–Kendall test

The Mann-Kendall test made it possible to detect possible gradual changes in the series of extreme variables. According to Mann (1945) and Kendall (1975), this non-parametric test, based on the rank, makes it possible to determine whether the correlation between time and the study variable is significant or not. Let (x 1,...., xn) be a sample of independent values relating to a random variable X whose stationarity we want to evaluate. The Mann-Kendall statistic is defined as follows:

$$S= \sum_{i=1}^{n-1}\sum_{j=i+1}^{n} \text{signe}\,(x_i-x_j) \quad \ldots \quad (21)$$

To determine the extent of the change, the method slope of the Sen (Sen, 1968) was applied and is obtained by the following formula (Equation 22):

$$b=\text{Mediane}\left[\frac{(X_j\text{-}X_i)}{(j\text{-}i)}\right],\ \text{pour } i<j \ \ldots\ldots\ldots\ldots\ldots (22)$$

Where b is the slope between the dots of data xj And Xi measured At time I And I respectively.

RESULTS AND DISCUSSION

Characteristics of the Calculated Hydrological Parameters

Annually

The main hydro-climatic parameters calculated over the periods 2021-2040, 2041-2060, 2061-2080, and 2081-2100 are the average annual rainfall (Pmm), the effective rainfall (Pe), the runoff potential (R), and the seepage potential (I). The statistical characteristics of these parameters are presented in Table 2. Figure 2 gives an overall view of the evolution of the parameters according to the periods (years) and according to the scenarios. Apart from the average temperature and PET which will increase over the years, ETR, precipitation, runoff potential (R), and infiltration potential (I) will decrease. The infiltration potential (I) will be even greater than the runoff potential (R).

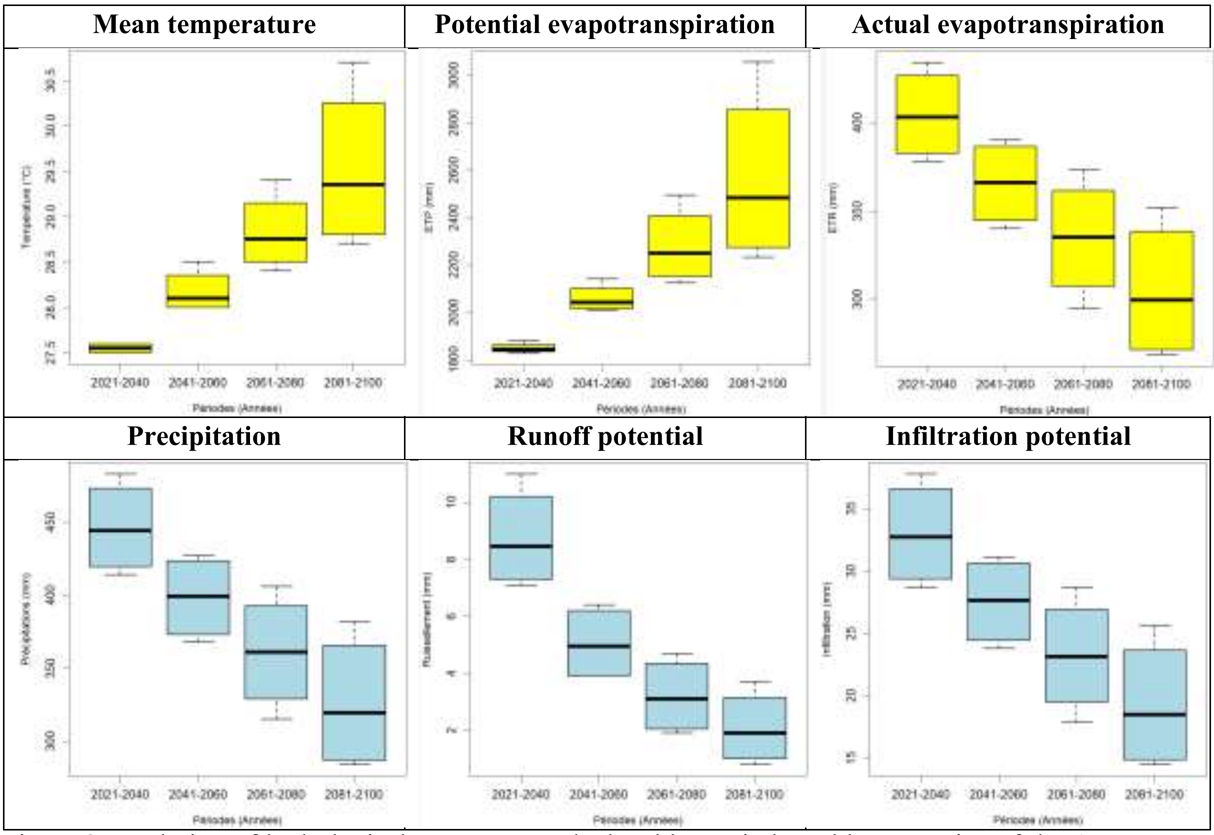

Figure 2. Evolution of hydrological parameters calculated by periods and by scenarios of the Aga- Foua - Djilas basin

The analysis of Table 2 shows significant fluctuations from one period to another and according to the scenarios. These will have considerable impacts on the environment and socio-economic activities in the Aga- Foua - Djilas basin.

Table 2. Statistical characteristics of the hydrological parameters calculated by scenario and by period in the Aga- Foua - Djilas basin

SSP 126	mmm	Temp	PET	ETo	Pe	R	I
2021-2040	463	27.6	1880	419	44.8	9.4	35.4
2041-2060	420	28.0	2021	383	36.2	6.0	30.2
2061-2080	379	28.4	2124	350	29.3	4.0	25.2
2081-2100	382	28.7	2232	352	29.4	3.7	25.6
SSP 245	Pmm	Temp	PET	ETo	Pe	R	I
2021-2040	483	27.5	1847	434	48.8	11.0	37.8
2041-2060	427	28.0	2009	390	37.6	6.4	31.1
2061-2080	406	28.6	2182	373	33.4	4.7	28.7
2081-2100	349	28.9	2318	325	24.4	2.6	21.7
SSP 370	Pmm	Temp	PET	ETo	Pe	R	I
2021-2040	414	27.5	1827	378	35.8	7.1	28.7
2041-2060	368	28.2	2063	340	27.7	3.9	23.8
2061-2080	315	28.9	2319	295	19.8	1.9	17.9
2081-2100	290	29.8	2652	274	16.4	1.2	15.3
SSP 585	Pmm	Temp	PET	ETo	Pe	R	I
2021-2040	425	27.6	1842	387	37.6	7.5	30.1
2041-2060	378	28.5	2141	349	29.0	3.9	25.1
2061-2080	343	29.4	2496	320	23.2	2.2	21.1
2081-2100	284	30.7	3059	269	15.3	0.8	14.5

Pmm: Mean annual rainfall (P), Temp: Average annual temperature, Pe: Effective rain (Pe); R: Runoff potential (R), I: Infiltration potential (I), PET: Actual evapotranspiration (ETO), PET: Potential evapotranspiration (PET)

Under the SSP 126 scenario, the average annual rainfall will drop from 463 mm in the near future to 382 mm in the distant future, i.e. a decrease of 21.2%. The average temperature will fluctuate. From 2021-2041 (27.6°C) to 2061-2080 (28.4°C), it will increase by 0.8°C and then by 1.1°C in 2081-2100 (28.7°C). At the same time, the PET will constantly increase during the different periods, while the other parameters (o, Pe, R, and I) will drop. From 1880 mm, the PET will exceed the 2000 mm mark from the mean future n°1 (2038) and reach 2232 mm in the distant future, that is to say, a rate of evolution of 18.7%. For the ETo, the model predicts a drop of 67 mm between the beginning and the end of the 21st century (419 mm in 2021-2041 and 352 mm in 2081-2100). In 2021-2040 (with 44.8 mm), effective rainfall will represent 9.7% of the average annual rainfall compared to 7.7% in 2081-2100 (29.4 mm). Runoff potential is less important than infiltration. It will increase from 9.4 mm in 2021-2040 to 3.7 mm in 2081-2100 when the infiltration potential will be 35.4 mm and 25.6 mm respectively for the same periods.

Under the SSP 245 scenario, the average annual rainfall forecast will be less than that under the SSP 126, except for the period 2041-2060 (427 mm against 420 mm). The drop in rain will be more intense there. It will be 27.7% between the near future (427 mm) and the distant future (349 mm). On the other hand, the average temperature will increase by 1.4°C between 2021-2040 (27.5°C) and 2081-2100 (28.9°C). This increase in the average temperature will have a considerable impact on the PET, which will constantly increase over time. It will experience a 25.5% increase between the beginning (1847 mm) and the end of the 21st century (2318 mm). The ETo, which will have an opposite pace to the PET, will represent 23.3% of the latter in 2021-2040 and 14.0% in 2081-2100. The effective rainfall will drop from 48.8 mm in 2021-2040 to 24.4 mm in 2081-2100, i.e. a drop of 50.0 mm. In relative value, the drop in runoff potential will be very significant. It will rise to 76.4% between the near future and the distant future. That of the infiltration potential will be less important. It is projected at 42.6% between these two periods.

Under the SSP 370 scenario, the average annual rainfall will be 414 mm during the first period of 2021-2040. The annual quantity of water expected with this scenario will continue to decrease over the years (368 mm in 2041-2060, 315 mm in 2061-2080, and 290 mm in 2081-2100). The predicted mean temperature is substantially equal to or even higher than that of SSP 245 between the near and mean future 1. However, from mean future 2, a net increase is expected (28.9°C) and will be accentuated at horizon 2100 (29.8°C). Regarding the PET, even if the SSP 370 scenario is more pessimistic than the 245 scenario, during the first study period, its value will be lower (1827 mm). The latter will increase by 825 mm in 2081-2100, an increase of 45.2%. The ETo, during the first period, will represent 20.7% of the PET against 10.3% in the distant future. As for the effective rain, for the same periods, it will increase from 35.8 mm to 16.4 mm, which represents respectively 8.6% and 5.7% of the average rain. The R and the I could reach lower values than those of the previous scenarios. In 2021-2040, 7.1 mm of runoff potential is expected against 28.7 mm of infiltration potential, 3.9 mm against 23.8 mm in 2041-2060, 1.9 mm against 17.9 mm in 2061-2080, and finally 1.2 mm against 15.3 mm in 2081-2100.

Under the SSP 585 scenario, the projected annual rainfall is greater during the first two periods than under the SSP 370 scenario, when it is the most pessimistic. Indeed, in 2021-2040, 2041-2060, and 2061-2080, the expected volume of water will be 425 mm, 378 mm, and 343 mm respectively. By 2100, it will be 284 mm, ie a rate of change of -33.2% between the near and distant future. Under this scenario, the thermal amplitude between the beginning and the end of the 21st century will be greater. An increase of 3.1°C in the average temperature is thus forecast (27.6°C in 2021-2040 against 30.7°C in 2081-2100). Like the average temperature, the PET will be much higher. From 1842 mm in 2021-2040, it will exceed 3000 mm in 2081-2100 (3059 mm). In 2021-2040 (387 mm) and 2041-2060 (349 mm), the ETo will be more intense under this scenario than under the SSP 370 scenario. It will gradually decrease during the last two periods ranging from 320 mm to 269 mm. This same state of the figure of the ETo prevails with the other hydrological parameters which are the Pe, the R, and the I. Between the beginning and the end of the century, the Pe will go from 37.6 mm to 15.3 mm; the R from 7.5 mm to 0.8 mm, and the I from 30.1 mm to 14.5 mm.

Monthly

Figure 3 shows an unimodal evolution of the simulated monthly rainfall as well as the runoff potential. The months of July, August, and September will be the wettest. In addition, it is during these months when the quantity of water received is greater that the runoff potential will be greater. The peak will always occur in August for both precipitation and runoff potential. The latter is largely dependent on rainfall in addition to PET. Over the years and the more the scenario is pessimistic, the monthly rainfall will decrease and the runoff potential will follow the same evolution. By 2100, the August runoff potential under the SSP 585 scenario will decline by almost 95%. This state of affairs deserves particular reflection for the implementation of adequate water management strategies in the watershed, which is highly agricultural.

Under the SSP 125 scenario, it is only in July of the 2021-2040 period that the bar of 100 mm of rain will be crossed (114.5 mm). In September too, it is during this first period that the bar of 180 mm will be exceeded (182). The volume of water expected in August will increase from 182 mm in 2021-2040 to 136 mm by 2100. For these same periods, the runoff potential for August will be 57.5 mm and 16. 0mm; a decrease of 72.1%.

Under the SSP 245 scenario, the expected precipitation in August (2041-2060) will be 171 mm. August will see its average rainfall drop between the beginning and the end of this 21st century (from 171 mm to 125 mm). It is the same for September whose rainfall will decrease between the near future (155 mm) and the distant future (112 mm). The runoff potential will follow this same state of affairs during these two months. In August, the runoff potential will therefore decrease by 76.3% between 2021-2040 (50.2 mm) and 2081-2100 (11.9 mm).

Under the SSP 370 scenario, rainfall on a monthly scale will be lower compared to the other scenarios. It is only the month of August that will record rain above 150 mm in the near future. Over the years, the rain will thus decrease and pass between the beginning and the end of the century from 66.5 mm to 44.1 mm in July, from 158 mm to 100 mm in August, and from 124 mm to 93.6 mm in September. Runoff potential under this scenario will not reach 5 mm in July (2.7 mm) of the first period, unlike the other scenarios. In August, the R forecast in 2021-2040 rises to 40.5 mm and will drop to 4.80 mm in 2081-2100, a decline of 88.1%.

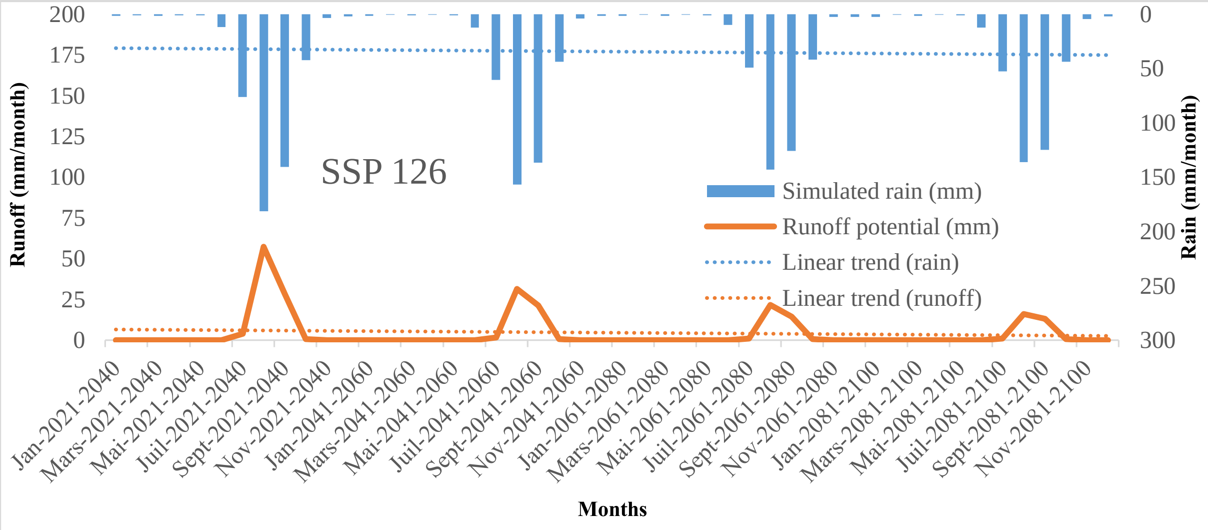

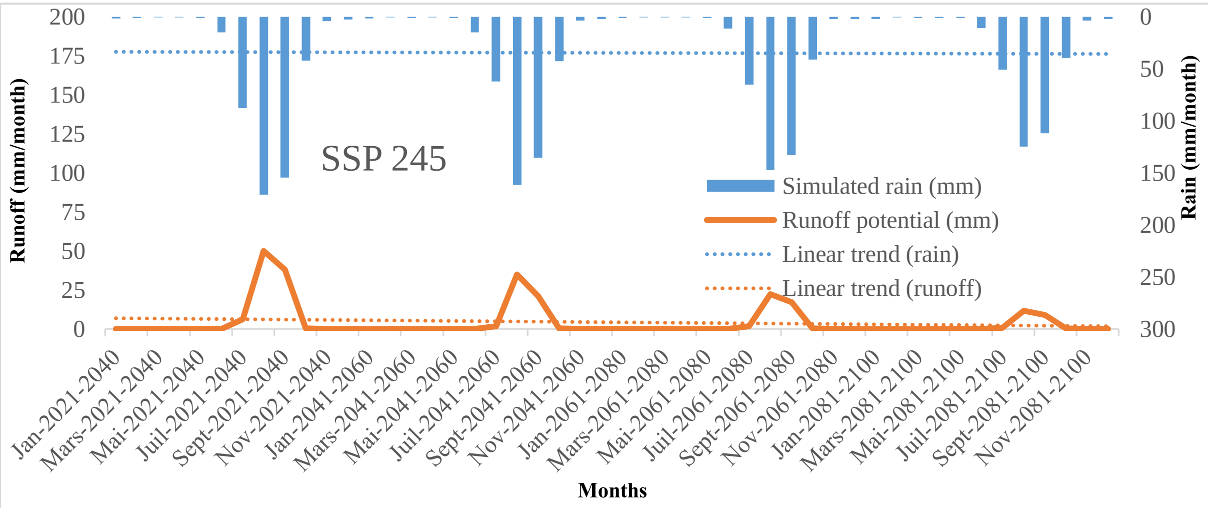

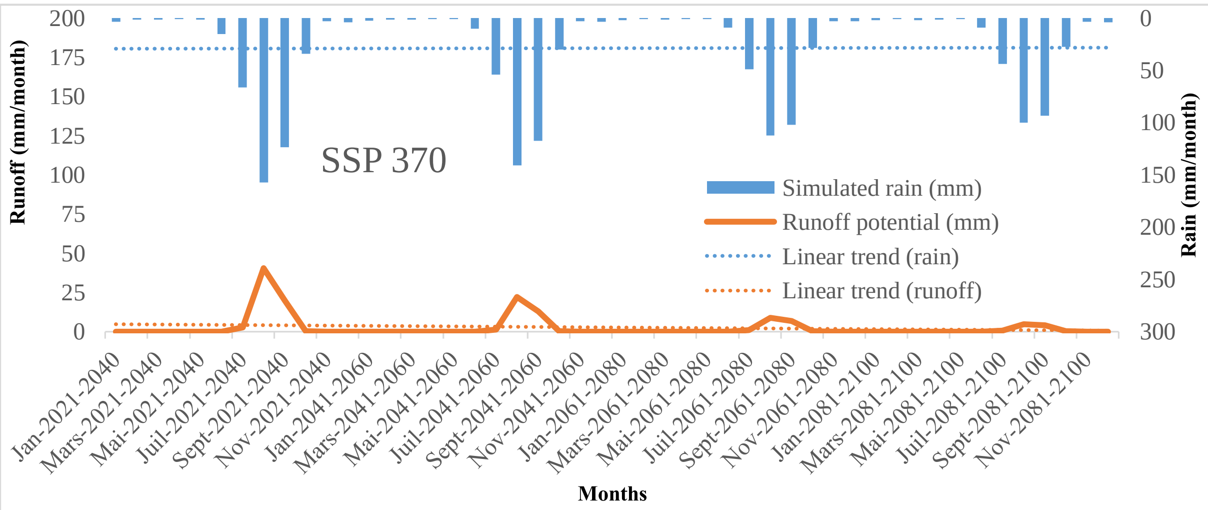

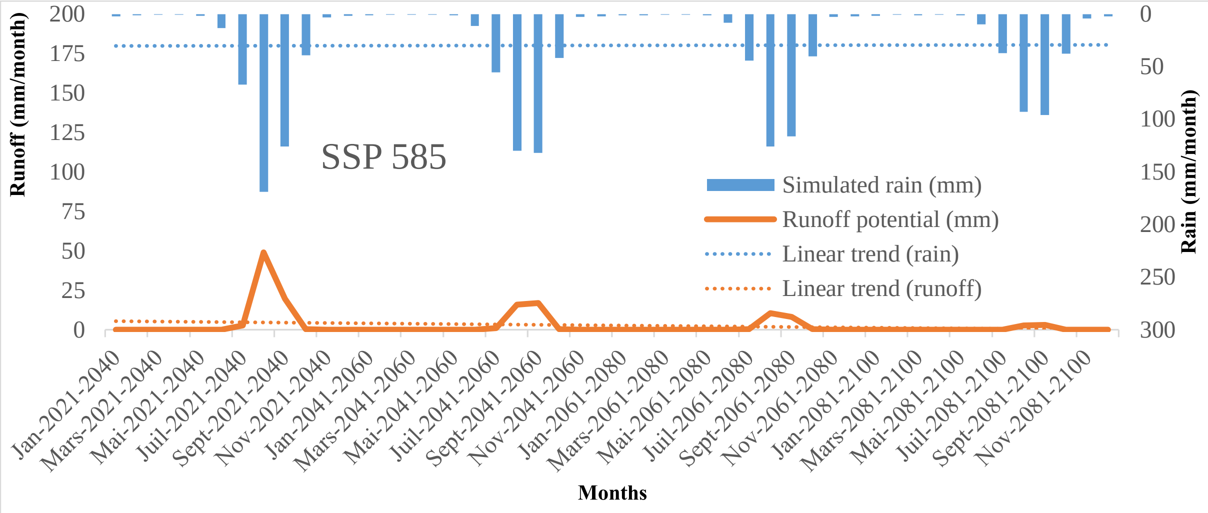

Figure 3. Comparative evolution of rainfall and runoff potential estimated by period and by scenario of the Aga- Foua - Djilas basin

Under the SSP 585 scenario, which is the most pessimistic scenario, during the near and medium future, the expected rainfall will be significantly higher than that of the SSP 370 scenario; which will be the same case for the runoff potential. It is expected in July, August, and September 2021-2040 respectively 66.2, 169, and 126 mm of rain. It is only this scenario that projects an R approaching 50mm in August in the near future (49.1mm). In August, the R will decrease from 49.1 mm in 2021-2040 to 2.81 mm in 2081-2100, a decrease of 94.2%.

The climate trends calculated based on the SSP scenarios in this research are aligned with previous research around Senegal (Mbaye et al., 2019; Sadio et al., 2020; Diakhaté et al., 2022) as well as outside (Almazroui et al. 2021; Diaz et al. 2020; Ortega et al. 2021; Phan and Nguyen, 2023). The results are different from the results where a statistically insignificant upward trend in precipitation was recorded in all seasons (including the annual time scale) (Girma et al., 2016) and statistically significant in July and November (Arragaw and Woldeamlak, 2017) in the central highlands of Ethiopia have been reported.

Assessment of dry conditions in the basin

To better understand the future conditions of the drought in the Aga- Foua - Djilas basin, the severity levels of the latter are analyzed in this part thanks to the SPEI and SPI. To check the trends in the time series and identify possible break periods, Mann-Kendall's and Pettitt's tests are respectively applied to the data. The scenarios retained are the SSP 245, the intermediate scenario, and the SSP 585, the most pessimistic scenario in terms of climate resilience.

The results are recorded in Table 3 and show significant fluctuations. Man Kendall's test indicates a downward trend in SPEI and SPI under all scenarios. The downward trend is most significant below SSP 585 for SPEIs and most significant below SSP 245 for SPIs. For SPEI, Kendall's tau is -0.490, -0.577, -0.674, and -0.769 respectively for SPEI 3, SPEI 6, SPEI 12 and SPEI 24 under SSP 245, and -0.660, -0.722, -0.781 and - 0.856 respectively for SPEI 3, SPEI 6, SPEI 12 and SPEI 24 under SSP 585. For SPI, Kendall's tau, always negative, is less significant, compared to SPEI. It is -0.167, -0.268, -0.434, and -0.529 respectively for SPI 3, SPI 6, SPI 12, and SPI 24 under SSP 245, and -0.148, -0.228, -0.337 and -0.447 respectively for SPI 3, SPI 6, SPI 12 and SPI 24 under SSP 585.

Pettitt test, meanwhile, reveals the presence of years of rupture. The latter will be earlier under the SSP 585 scenario than under the SSP 245 (Table 3).

Under the SSP 245 scenario, the rupture will occur for SPEI 3 and SPEI 6 respectively in February and April 1967 and in August of the same year for SPEI 12. In April of the following year, the rupture of SPEI 24 will occur. From July 2070, SPI 6 and 24 will experience a rupture, this will occur more for SPI I2 (in July 2069) and later for SPI 3 (in October 2071). Under the SSP 585 scenario where the rupture is earlier, the SPEI 3 will record it in November 2061, the SPEI 6 (in February) and SPEI 12 (in June), and the SPEI 24 (in November) in 2062. For SPIs, ruptures are scheduled for April (for SPI 3), May (for SPI 6), and August (for SPI 12) of the year 2065, and July (for SPI 24) of the year 2066. For the SPEI as for the SPI, the ruptures under the SSP 585 scenario are planned for one to two years.

Table 3. Man Kendall test and Pettitt test on SPEI and SPI by scenario over the period 2021-2100 in the Aga- Foua - Djilas basin

				Man Kendall test				
SSP 245	**SPEI3**	**SPEI6**	**SPEI12**	**SPEI24**	**SPI3**	**SPI6**	**SPI12**	**SPI24**
Kendall's Tau	-0.490	-0.577	-0.674	-0.769	-0.167	-0.268	-0.434	-0.529
p-value	< 0.0001	< 0.0001	< 0.0001	< 0.0001	< 0.0001	< 0.0001	< 0.0001	< 0.0001
alpha	0.05	0.05	0.05	0.05	0.05	0.05	0.05	0.05
Sen slope	-0.002	-0.003	-0.003	-0.003	-0.0008	-0.002	-0.002	-0.003
SSP 585	**SPEI3**	**SPEI6**	**SPEI12**	**SPEI24**	**SPI3**	**SPI6**	**SPI12**	**SPI24**
Tau de Kendall	-0.660	-0.722	-0.781	-0.856	-0.148	-0.228	-0.337	-0.447
p-value	< 0.0001	< 0.0001	< 0.0001	< 0.0001	< 0.0001	< 0.0001	< 0.0001	< 0.0001
alpha	0.05	0.05	0.05	0.05	0.05	0.05	0.05	0.05
Pente de Sen	-0.003	-0.003	-0.003	-0.003	-0.0007	-0.001	-0.002	-0.002
				Test de Pettitt				
SSP 245	**SPEI3**	**SPEI6**	**SPEI12**	**SPEI24**	**SPI3**	**SPI6**	**SPI12**	**SPI24**
Breakup date	2067-02	2067-04	2067-08	2068-04	2071-10	2070-07	2069-07	2070-07
p-value	< 0.0001	< 0.0001	< 0.0001	< 0.0001	< 0.0001	< 0.0001	< 0.0001	< 0.0001
Average before break	0.41	0.47	0.53	0.59	0.19	0.28	0.40	0.48
Average after break	-0.76	-0.85	-0.93	-1.01	-0.3	-0.48	-0.68	-0.83
Variation rate	-154	-156	-157	-159	-163	-158	-159	-158
SSP 585	**SPEI3**	**SPEI6**	**SPEI12**	**SPEI24**	**SPI3**	**SPI6**	**SPI12**	**SPI24**
Date de rupture	2061-11	2062-02	2062-06	2062-11	2065-04	2065-05	2065-08	2066-07
p-value	< 0.0001	< 0.0001	< 0.0001	< 0.0001	< 0.0001	< 0.0001	< 0.0001	< 0.0001
Average before break	0.59	0.62	0.64	0.67	0.17	0.25	0.35	0.43
Average after break	-0.83	-0.88	-0.91	-0.93	-0.24	-0.39	-0.57	-0.73
Variation rate	-170	-170	-171	-172	-170	-164	-161	-159

For all scenarios, the pre-rupture period is much more characterized by mild humidity and the post-rupture period by mild drought. The rate of variation between the pre and post-rupture periods is higher under the SSP 585 scenario, which is more pessimistic. The SPEIs will record the highest rates of variation. These are respectively -154, -156, -157 and -159% for SPEI 3, 6, 12 and 24 under the SSP 245 scenario, and -170% (SPEI 3 and 6, -171% (SPEI 12) and -172% (SPEI 24) under the SSP 585 scenario. The SPIs with lower rates of change will record the most drastic deficit with the SPI 3 (-163% under the SSP 245 and -170% under the SSP 585).

This trend and noted break dates are illustrated in Figures 4 to 7 which show the time course of projected wetness and dryness at the basin outlet from 2021 to 2100 and under the SSP 245 and 585 scenarios. The analysis of these figures reveals two distinct phases: a first marked by the domination of humidity and which extends from 2021 to the 2060s; a second dominated by drought and ranging from the middle to the end of the 21st century.

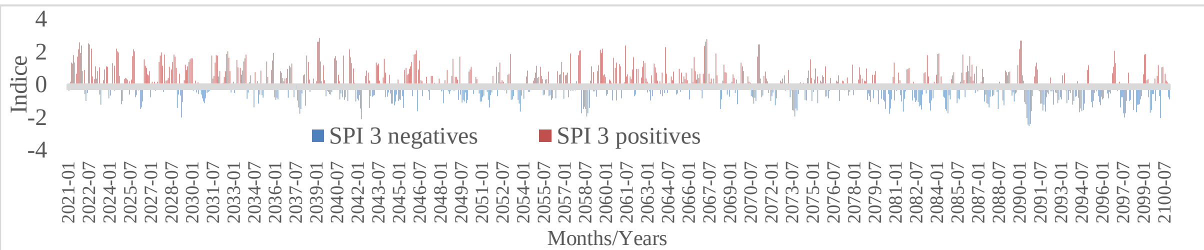

Figure 4. Projected humidity and drought at the outlet of the Aga- Foua - Djilas basin from 2021 to 2100 under the SSP 245 scenario from the SPI at different time scales

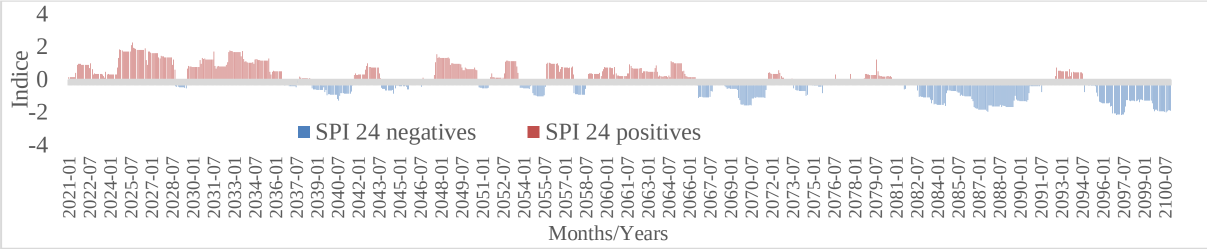

Figure 5. Projected humidity and drought at the outlet of the Aga- Foua - Djilas basin from 2021 to 2100 under the SSP 585 scenario from the SPI at different time scales

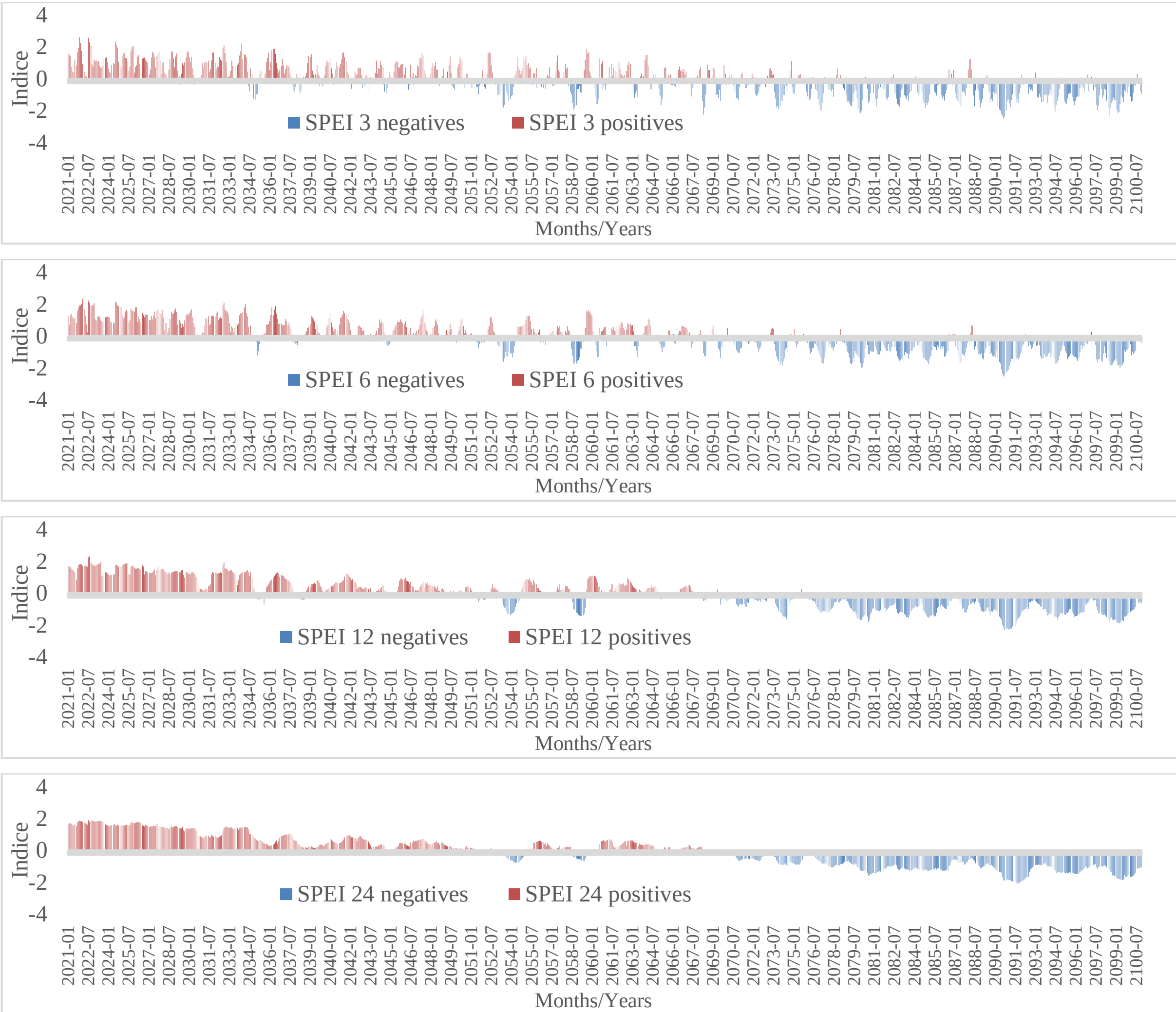

Figure 6. Projected humidity and drought at the outlet of the Aga- Foua - Djilas basin from 2021 to 2100 under the SSP 245 scenario from the SPEI at different time scales

Tables 4 and 5 show the distribution of the percentages of dry and wet sequences from the SPEI and SPI by scenario and over the study period. Overall, the projected data predicts more frequent mild drought hazards and followed by mild wet spells. These frequencies of dry and wet light occurrences are greater than or equal to 30% under all scenarios, except for SPEI 24 under SSP 245 and SPEI 12 and SPEI 24 under SSP 585. With this last scenario, SPI 24 could approach 40%.

Figure 7. Projected humidity and drought at the outlet of the Aga- Foua - Djilas basin from 2021 to 2100 under the SSP 585 scenario from the SPEI at different time scales

Table 4. Percentage of dry and wet sequences from SPEI and SPI by scenario over the period 2021-2100 in the Aga- Foua - Djilas basin

SSP 245	SPEI3	SPEI6	SPEI12	SPEI24	SPI3	SPI6	SPI12	SPI24
Extremely wet	1.15	0.94	0.21	0.00	3.23	2.92	2.19	1.46
Severely wet	3.96	4.58	5.63	8.13	5.10	6.04	4.69	9.06
Moderately wet	10.10	10.31	11.5	7.0	7.81	7.92	8.54	4.90
slightly wet	31.1	30.5	29.6	35.9	32.0	31.3	32.8	34.3
slightly dry	34.5	33.5	32.0	27.6	38.4	34.7	32.9	32.8
Moderately dry	12.1	13.4	15.8	16.1	8.9	11.6	11.7	12.2
Severely dry	5.73	5.73	4.06	4.58	3.75	4.58	5.83	3.96
extremely dry	1.35	0.94	1.25	0.63	0.83	1.04	1.35	1.35
Total	100	100	100	100	100	100	100	100
SSP 585	SPEI3	SPEI6	SPEI12	SPEI24	SPI3	SPI6	SPI12	SPI24
Extremely wet	0.21	0.00	0.00	0.00	2.50	1.35	0.73	0.21
Severely wet	2.50	2.40	1.88	1.46	5.10	5.83	5.83	4.58
Moderately wet	11.1	10.5	10.8	11.8	9.06	8.23	7.40	9.06

slightly wet	33.5	34.0	34.9	37.1	29.0	32.3	35.3	34.3
slightly dry	32.4	32.0	28.9	26.8	39.2	34.3	33.1	32.5
Moderately dry	12.0	12.8	15.3	13.4	10.94	12.0	9.4	10.7
Severely dry	7.81	8.02	8.02	9.48	3.96	5.63	8.23	7.50
extremely dry	0.42	0.31	0.21	0.00	0.31	0.42	0.00	1.15
Total	100	100	100	100	100	100	100	100

After the light dry and wet sequences, the moderate dry and wet ones will be respectively more frequent. They will record significant rates ranging from 4.90% (for SPI 24, under SSP 245) to 16.1% (SPEI 24, under SSP 585). Under SSP 245, severe drought and humidity will counterbalance each other with frequencies not exceeding 9%. On the other hand, under SSP 585, occurrences of severe drought will be more frequent than wet ones, except for SPI 3 (3.96% against 5.10%) and SPI 6 (5.63% against 5, 83%). The occurrence of these severe occurrences will be less frequent with rates ranging from 1.46% (SPEI 24) to 5.83% (SPI 6) in the wet phase and from 3.96% (SPI 3) to 9.48% (SPI 24) in the dry phase.

In terms of cumulative wet occurrences and dry occurrences, Table 5 shows a reversal of the situation from the near future to the distant future and from the optimistic scenario to the pessimistic one. The near future will indeed be marked by wet occurrences. In the mean future 1, the dry sequences will increase and exceed those wet in the mean future 2. The distant future will be considerably dominated by drought.

Table 5. Percentage of accumulations of dry and wet sequences from SPEI and SPI by scenario and by period in the Aga- Foua - Djilas basin

					SSP 245				
2021-2040	SPEI3	SPEI6	SPEI12	SPEI24	2021-2040	SPI3	SPI6	SPI12	SPI24
Humid	54.2	56.7	56.3	60.4	Humid	60.8	64.2	75.8	85.8
dry	45.8	43.3	43.8	39.6	Sec	39.2	35.8	24.2	14.2
2041-2060	SPEI3	SPEI6	SPEI12	SPEI24	2041-2060	SPI3	SPI6	SPI12	SPI24
Humid	52.9	56.7	56.7	54.2	Humid	46.3	46.3	40.0	40.8
dry	47.1	43.3	43.3	45.8	Sec	53.8	53.8	60.0	59.2
2061-2080	SPEI3	SPEI6	SPEI12	SPEI24	2061-2080	SPI3	SPI6	SPI12	SPI24
Humid	22.1	22.1	22.9	8.8	Humid	53.8	59.6	67.1	67.1
dry	77.9	77.9	77.1	91.3	Sec	46.3	40.4	32.9	32.9
2081-2100	SPEI3	SPEI6	SPEI12	SPEI24	2081-2100	SPI3	SPI6	SPI12	SPI24
Humid	5.0	1.3	0.4	0.0	Humid	31.7	22.5	10.0	5.0
dry	95.0	98.8	99.6	100.0	Sec	68.3	77.5	90.0	95.0
					SSP 585				
2021-2040	SPEI3	SPEI6	SPEI12	SPEI24	2021-2040	SPI3	SPI6	SPI12	SPI24
Humid	92.5	96.3	99.2	100.0	Humid	51.7	61.3	69.6	77.5
dry	7.5	3.8	0.8	0.0	Sec	48.3	38.8	30.4	22.5
2041-2060	SPEI3	SPEI6	SPEI12	SPEI24	2041-2060	SPI3	SPI6	SPI12	SPI24
Humid	72.1	71.7	75.4	87.9	Humid	50.8	59.2	62.1	58.8
dry	27.9	28.3	24.6	12.1	Sec	49.2	40.8	37.9	41.3
2061-2080	SPEI3	SPEI6	SPEI12	SPEI24	2061-2080	SPI3	SPI6	SPI12	SPI24
Humid	24.6	19.6	15.8	13.3	Humid	47.1	46.7	51.3	45.8
dry	75.4	80.4	84.2	86.7	Sec	52.9	53.3	48.8	54.2
2081-2100	SPEI3	SPEI6	SPEI12	SPEI24	2081-2100	SPI3	SPI6	SPI12	SPI24
Humid	0.4	0.0	0.0	0.0	Humid	32.9	23.8	14,2	10,4
dry	99,6	100,0	100,0	100,0	Sec	67,1	76,3	85,8	89,6

Under SSP 245, wet occurrences will dominate the seasons for the near future. With a frequency above 55% and reaching 60.4% (SPEI 24), the SPEI will see its shares drop slightly by less than 2% (on the 3, 6 and 12-month scales) and 6% (on the 24 months) in 2041-2060. The SPEI continues to have the highest frequencies there for the wet phases, while the SPIs already display wet sequences lower than the dry ones. SPI values will fall by 14.5 to 35.8% (on the 3, 6, and 12 month scales) and by 45% (on the 24 month scale) at mean future 1. At mean future 2, the trend will also be reversed for SPEI. Dry occurrences will be the most frequent. With the SPEI, they will represent more than ¾ of the frequencies and more than half with the SPI. At the end of the 21st century, the drought will be perennial in the basin. Thus, the dry occurrences of SPEI could exceed 95% (on the 3, 6, and 12-month scales) and reach 100% (on the 24 month scale). For the SPI, the dry periods will represent more than ¾ of the frequencies and will be 89.6% with the SPI 24.

Under SSP 585, the period (2021-2040) will be more marked by wet occurrences, even if this scenario is more pessimistic than SSP 245. Indeed, with SPEIs, 92.5% of wet phases are expected for the 3-month scale and from 96.3 to 100% for the other scales (6, 12, and 24 month scales). These wet occurrences, although greater than the dry ones, will be less frequent under the SPI (on the 3, 6, and 12 month scales) compared to the SPEI. They will fluctuate between 51.7% (on the 3-month scale) and 77.5% (on the 24-month scale). Over the years, the trend will reverse, as is the case under the SSP 245. In the mean future 1, the frequency of dry occurrences will increase but will be less important under this scenario than under the more optimistic SSP 245. The dry sequences will always be more frequent and will represent more than ¾ of the frequencies with the SPEI and half with the SPI. It will be necessary to reach the future average of 2 to witness a more assiduous frequency of drought with rates higher than those will that could be recorded under SSP 245. The SPEI will thus have frequencies of 75.4% (3), 80.4 % (6), 84.2% (12), 86.7% (24).

The SPI will see increases of 4.6% (on the 3-month scale), 14.5% (over 6 months), 18.4% (over 12 months) and 31.7% (over 24 months). By 2100, for SPEI, only SPEI 3 could have 0.4% wet occurrences. Everything else will be marked by drought. For the SPI, the wet sequences, although much lower than the dry ones, will be quite significant with the SPEI 3 (32.9%), the SPEI 6 (23.8%), the SPEI 12 (14.2%), and the SPEI 24 (10.4%) and will exceed those below the SSP 245.

To understand the future drought characteristics, this study also compared the results of the time series of the SPI and SPEI drought indices for the scenarios SSP 245 and SSP 585 for the period from 2021 to 2100. The SPEI shows more drought conditions in the future with respect to SPI suggesting an increase in PET with respect to precipitation. In addition, the drought zone in the Aga- Foua - Djilas basin is likely to increase at the end of the 21st century with values around 80 % for SPI and 90% for SPEI under the scenarios SSP 245 and SSP 585. Projected drought results from SPEI and SPI show an increase in drought conditions throughout the 21st century in the SSP scenarios considered. Future drought changes were detected using time scales such as drought area, different levels of drought severity (moderate, severe, and extreme), and different times using monthly and seasonal. The projected change in the drought zone showed an increase in all SSPs and all times. Specifically, the predicted change in drought zones is projected to show a large increase by the end of the 21st century. These suggest that the basin will face unprecedented increases in drought area by the end of the 21st century under the SSP 585 scenario if drought mitigation and adaptation mechanisms are inadequate.

In many studies (Ahmadalipour et al., 2017; Feng et al., 2017; Nguvava et al., 2019; Spinoni et al., 2020) on drought assessment using SPI and SPEI, we note a large difference in the magnitude and direction of the phenomenon. For example, in the East African region, Nguvava et al. (2019) revealed that SPEI simulated higher drought magnitude than SPI. If we only use precipitation to make drought projections, we see a decrease in drought in the basin, unlike using both precipitation and PET, two parameters to use to calculate the SPEI (Spinoni et al ., 2020). With all of this, SPEI is therefore considered more robust to detect possible future risks of drought in the context of global warming. This is why Nguvava et al. (2019) indicated that incorporating PET into quantifying the severity of future drought projections is better than using precipitation alone. To this end, the use of SPEI for drought projection is advantageous to understanding future drought changes in the basin to minimize them.

CONCLUSION

Senegal is vulnerable to climate variability, and climate change is likely to increase the frequency and magnitude of disasters. The adverse effects of climate change can aggravate existing social and economic problems across the country, especially where people depend on climate-sensitive resources and rain-fed agriculture. This study was undertaken to analyze the hydrological impacts of climate change (temperature and precipitation) in the Aga- Foua - Djilas basin, over the future period 2021-2100 using CMIP6 projections under SSP 126, SSP 245, SSP 370, and SSP 585. In sum, the study of the future climate in the Aga- Foua - Djilas basin reveals temperatures and rising PET, rainfall, runoff potential, and falling infiltration potential, regardless of the projection scenario, optimistic or pessimistic.

Regarding the drought analysis, the SPEI shows more drought conditions in the future compared to the SPI in the Aga- Foua - Djilas basin. Thus, future drought risks can be minimized by incorporating PET data into drought quantification rather than using precipitation alone in the context of global warming. The predicted change in the drought zone showed an increase in all SSPs and periods in the basin. By the end of the 21st century, the drought zone is expected to increase much more below SSP 585, respectively. Drought event, duration, frequency, and intensity showed increasing patterns of drought spatial change with increasing periods under all SSPs with exceptions in drought event changes. Analysis of uncertainty of climate change affects drought patterns shows that projected changes in drought are likely to increase under higher uncertainties with increasing time intervals between the near future and the end of the 21st century.

Based on this knowledge of the future climate, it is important to assess the basin's water resources in the short, medium, and long term. This will help to better refine sustainable water management strategies and guide public agricultural policies. In addition, projecting drought spread over different future times is important for policymaking, infrastructure decisions, and overall monitoring of climate change impacts on drought. Projected drought conditions are essential for the development of drought adaptation and mitigation policies. This study has created a good overview for understanding likely future drought conditions in the Aga- Foua - Djilas basin. The results of this study provide important implications for climate change adaptation scenarios and territorial planning in the Sahelian environment. The methodology developed in this study can be used for reliable projections of future climate characteristics in any basin, and the results can be used in the development of adaptation and mitigation plans in Senegal. Future farm management strategies should also consider possible future conditions.

REFERENCES

Abramowitz, M., & Stegun, I. A. (1965). *Handbook of Mathematical Functions: With Formulas, Graphs, and Mathematical Tables*. Courier Corporation.

Ahmadalipour, A., Moradkhani, H., & Demirel, M. C. (2017). A comparative assessment of projected meteorological and hydrological droughts: Elucidating the role of temperature. *Journal of Hydrology*, *553*, 785–797.

Alemayehu, A., & Bewket, W. (2017). Smallholder farmers' coping and adaptation strategies to climate change and variability in the central highlands of Ethiopia. *Local Environment*, *22*(7), 825–839.

Almazroui, M., Ashfaq, M., Islam, M. N., Rashid, I. U., Kamil, S., Abid, M. A., O'Brien, E., Ismail, M., Reboita, M. S., Sörensson, A. A., Arias, P. A., Alves, L. M., Tippett, M. K., Saeed, S., Haarsma, R., Doblas-Reyes, F. J., Saeed, F., Kucharski, F., Nadeem, I., … Sylla, M. B. (2021). Assessment of CMIP6 Performance and Projected Temperature and Precipitation Changes Over South America. *Earth Systems and Environment*, *5*(2), 155–183.

Ardoin-Bardin, S. (2004). *Variabilité hydroclimatique et impacts sur les ressources en eau de grands bassins hydrographiques en zone soudano-sahélienne* [PhD Thesis].

Ault, T. R., Mankin, J. S., Cook, B. I., & Smerdon, J. E. (2016). Relative impacts of mitigation, temperature, and precipitation on 21st-century megadrought risk in the American Southwest. *Science Advances*, *2*(10), e1600873.

Beguería, S., Vicente-Serrano, S. M., Reig, F., & Latorre, B. (2014). Standardized precipitation evapotranspiration index (SPEI) revisited: Parameter fitting, evapotranspiration models, tools, datasets and drought monitoring. *International Journal of Climatology*, *34*(10), 3001–3023.

Butu, H. M., Seo, Y., & Huh, J. S. (2020). Determining Extremes for Future Precipitation in South Korea Based on RCP Scenarios Using Non-Parametric SPI. *Sustainability*, *12*(3), 963.

Chen, J., Brissette, F. P., Lucas-Picher, P., & Caya, D. (2017). Impacts of weighting climate models for hydro-meteorological climate change studies. *Journal of Hydrology*, *549*, 534–546.

Chen, J., Brissette, F. P., Poulin, A., & Leconte, R. (2011). Overall uncertainty study of the hydrological impacts of climate change for a Canadian watershed. *Water Resources Research*, *47*(12), 2011WR010602.

Diakhaté, M., Mbaye, M. L., Camara, I., & Barry, M. B. (2022). Projected Changes in the Rainfall Annual Cycle over the Senegal River Basin Using CMIP5 bias-Corrected Simulations. *American Journal of Environmental Protection*, *10*(1), Article 1.

Díaz, L. B., Saurral, R. I., & Vera, C. S. (2021). Assessment of South America summer rainfall climatology and trends in a set of global climate models large ensembles. *International Journal of Climatology*, *41*(S1).

FAO (Ed.). (2017). *Building resilience for food and food security*. FAO.

Feng, H., & Zhang, M. (2015). Global land moisture trends: Drier in dry and wetter in wet over land. *Scientific Reports*, *5*(1), 18018.

Feng, S., Trnka, M., Hayes, M., & Zhang, Y. (2017). Why Do Different Drought Indices Show Distinct Future Drought Risk Outcomes in the U.S. Great Plains? *Journal of Climate*, *30*(1), 265–278.

Frasson, R. P. D. M., Pavelsky, T. M., Fonstad, M. A., Durand, M. T., Allen, G. H., Schumann, G., Lion, C., Beighley, R. E., & Yang, X. (2019). Global Relationships Between River Width, Slope, Catchment Area, Meander Wavelength, Sinuosity, and Discharge. *Geophysical Research Letters*, *46*(6), 3252–3262.

Fujimori, S., Hasegawa, T., Krey, V., Riahi, K., Bertram, C., Bodirsky, B. L., Bosetti, V., Callen, J., Després, J., Doelman, J., Drouet, L., Emmerling, J., Frank, S., Fricko, O., Havlik, P., Humpenöder, F., Koopman, J. F. L., Van Meijl, H., Ochi, Y., … Van Vuuren, D. (2019). A multi-model assessment of food security implications of climate change mitigation. *Nature Sustainability*, *2*(5), 386–396.

Fung, K. F., Huang, Y. F., Koo, C. H., & Soh, Y. W. (2020). Drought forecasting: A review of modelling approaches 2007–2017. *Journal of Water and Climate Change*, *11*(3), 771–799.

Girma, E., Tino, J., & Wayessa, G. (2016). Rainfall trend and variability analysis in Setema-Gatira area of Jimma, Southwestern Ethiopia. *African Journal of Agricultural Research*, *11*(32), 3037–3045.

Granderson, A. A. (2014). Making sense of climate change risks and responses at the community level: A cultural-political lens, Climate Risk Management, 3, 55-64.

IPCC (2021). Summary for Policymakers. In: Climate Change 2021: The Physical Science Basis. Contribution of Working Group I to the Sixth Assessment Report of the Intergovernmental Panel on Climate Change [MassonDelmotte, V., P. Zhai, A. Pirani, S. L. Connors, C. Péan, S. Berger, N. Caud, Y. Chen, L. Goldfarb, M. I. Gomis, M. Huang, K. Leitzell, E. Lonnoy, J.B.R. Matthews, T. K. Maycock, T. Waterfield, O. Yelekçi, R. Yu and B. Zhou (eds.)]. Cambridge University Press. In Press.

IPCC (Ed.). (2014). *Climate Change 2013 – The Physical Science Basis: Working Group I Contribution to the Fifth Assessment Report of the Intergovernmental Panel on Climate Change* (1st ed.). Cambridge University Press.

Javanmard, S. (2017). Spatial–Temporal Analysis of Drought in Iran Using SPI During a Long—Term Period. *Earth Sciences*, *6*(2), 15.

Kendall, M. G. (1975). *Multivariate analysis*. Griffin.

Konapala, G., Mishra, A. K., Wada, Y., & Mann, M. E. (2020). Climate change will affect global water availability through compounding changes in seasonal precipitation and evaporation. *Nature Communications*, *11*(1), 3044.

Kouamé, A. N., Amani, M. K., Gnaboa, R., Traoré, K. S., & Houenou, P. V. (2014). Analyse De Phenomènes Hydrologiques Dans Un Bassin Versant Urbanisé: Cas De La Ville De Yamoussoukro (Centre De La Cote D'ivoire). *LARHYSS Journal*, *17*, Article 17.

Kouassi, A. M., Assoko, A. V. S., Kouakou, K. E., Dje, K. B., Kouame, K. F., & Biemi, J. (2017). Analysis of the Hydrological Impacts of Climate Variability in West Africa: Case Study of the Bandama Watershed in Ivory Coast. *LARHYSS Journal*, *31*, Article 31.

Kouassi, A. M., N' Guessan, B., Kouame, K., Kouame, K., Okaingni, J., & Biemi, J. (n.d.). *Application of the cross-simulation method to the analysis of trends in the rainfall-flow relationship from the GR2M model: Case of N'zi -Bandama watershed (Ivory Coast). 344*, 288–296.

Laurent, L., Buoncristiani, J.-F., Pohl, B., Zekollari, H., Farinotti, D., Huss, M., Mugnier, J.-L., & Pergaud, J. (2020). The impact of climate change and glacier mass loss on the hydrology in the Mont-Blanc massif. *Scientific Reports*, *10*(1), 10420.

Leng, G., Tang, Q., & Rayburg, S. (2015). Climate change impacts on meteorological, agricultural and hydrological droughts in China. *Global and Planetary Change*, *126*, 23–34.

Leone, F., Meschinet De Richemond, N. & Vinet, F. (2010). Aléas naturels et gestion des risques. Paris, Presses Universitaires de France.

Lubes-Niel, H., Masson, J. M., Paturel, J. E., & Servat, É. (1998). *Climatic variability and statistics. Study by simulation of the power and the robustness of some tests used to check the homogeneity of chronicles. 3*, 383–408.

Mahe, G., Paturel, J.-E., Servat, E., Conway, D., & Dezetter, A. (2005). The impact of land use change on soil water holding capacity and river flow modelling in the Nakambe River, Burkina-Faso. *Journal of Hydrology*, *300*(1–4), 33–43.

Mann, H. B. (1945). Nonparametric Tests Against Trend. *Econometrica*, *13*(3), 245.

Mbaye, I., Sane, T., & Dieye, E. (2011, July 7). *Climate change, perceptions and strategies of the populations of the city of ziguinchor in Senegal*. Proceedings of the colloquium "Strengthening the resilience to climate change of cities: from spatial diagnosis to adaptation measures" (2R2CV), Paul Verlaine University - Metz, France.

Mbaye, M. L., Sylla, M. B., & Tall, M. (2019). Impacts of 1.5 and 2.0 °C Global Warming on Water Balance Components over Senegal in West Africa. *Atmosphere*, *10*(11), 712.

Milly, P. C. D., Dunne, K. A., & Vecchia, A. V. (2005). Global pattern of trends in streamflow and water availability in a changing climate. *Nature*, *438*(7066), 347–350.

Nguvava, M., Abiodun, B. J., & Otieno, F. (2019a). Projecting drought characteristics over East African basins at specific global warming levels. *Atmospheric Research*, *228*, 41–54.

Nguvava, M., Abiodun, B. J., & Otieno, F. (2019b). Projecting drought characteristics over East African basins at specific global warming levels. *Atmospheric Research*, *228*, 41–54.

Ortega, G., Arias, P. A., Villegas, J. C., Marquet, P. A., & Nobre, P. (2021). Present‐day and future climate over central and South America according to CMIP5 / CMIP6 models. *International Journal of Climatology*, *41*(15), 6713–6735.

Osima, S., Indasi, V. S., Zaroug, M., Endris, H. S., Gudoshava, M., Misiani, H. O., Nimusiima, A., Anyah, R. O., Otieno, G., Ogwang, B. A., Jain, S., Kondowe, A. L., Mwangi, E., Lennard, C., Nikulin, G., & Dosio, A. (2018). Projected climate over the Greater Horn of Africa under 1.5 °C and 2 °C global warming. *Environmental Research Letters*, *13*(6), 065004.

Pettitt, A. N. (1979). A Non-Parametric Approach to the Change-Point Problem. *Applied Statistics*, *28*(2), 126.

Phan, T. T. H., & Nguyen, H. A. (2023). Spatial and temporal distributions of temperature and rainfall on tropical islands of Vietnam. *Journal of Water and Climate Change*, *14*(5), 1395–1412.

Saada, N., & Abu-Romman, A. (2017). Multi-site Modeling and Simulation of the Standardized Precipitation Index (SPI) in Jordan. *Journal of Hydrology: Regional Studies*, *14*, 83–91.

Sadio, P. M., Mbaye, M. L., Diatta, S., & Sylla, M. B. (2020). Variabilité et changement hydroclimatiques dans le bassin-versant du fleuve Casamance (Sénégal). *La Houille Blanche*, *106*(6), 89–96.

Sen, P. K. (1968). Estimates of the Regression Coefficient Based on Kendall's Tau. *Journal of the American Statistical Association*, *63*(324), 1379–1389.

Servat, E., Paturel, J.-E., Kouame, B., Travaglio, M., Ouedraogo, M., Boyer, O., Lubes-Niel, H., Fritsch, J.-M., Masson, J.-M., & Marieu, B. (n.d.). *Identification, caractérisation et conséquences d'une variabilité hydrologique en Afrique de l'Ouest et centrale*.

Shiferaw, A., Tadesse, T., Rowe, C., & Oglesby, R. (2018). Precipitation Extremes in Dynamically Downscaled Climate Scenarios over the Greater Horn of Africa. *Atmosphere*, *9*(3), 112.

Spinoni, J., Barbosa, P., Bucchignani, E., Cassano, J., Cavazos, T., Christensen, J. H., Christensen, O. B., Coppola, E., Evans, J., Geyer, B., Giorgi, F., Hadjinicolaou, P., Jacob, D., Katzfey, J., Koenigk, T., Laprise, R., Lennard, C. J., Kurnaz, M. L., Li, D., … Dosio, A. (2020). Future Global Meteorological Drought Hot Spots: A Study Based on CORDEX Data. *Journal of Climate*, *33*(9), 3635–3661.

Sultan, B., & Janicot, S. (2006). *Climate and agriculture in West Africa*. *5*, 50–51.

Tang, Q. (2020). Global change hydrology: Terrestrial water cycle and global change. *Science China Earth Sciences*, *63*(3), 459–462.

Thornthwaite, C. W. (1948). An Approach toward a Rational Classification of Climate. *Geographical Review*, *38*(1), 55.

Touma, D., Ashfaq, M., Nayak, M. A., Kao, S.-C., & Diffenbaugh, N. S. (2015). A multi-model and multi-index evaluation of drought characteristics in the 21st century. *Journal of Hydrology*, *526*, 196–207.

Van Vuuren, D. P., Edmonds, J., Kainuma, M., Riahi, K., Thomson, A., Hibbard, K., Hurtt, G. C., Kram, T., Krey, V., Lamarque, J.-F., Masui, T., Meinshausen, M., Nakicenovic, N., Smith, S. J., & Rose, S. K. (2011). The representative concentration pathways: An overview. *Climatic Change*, *109*(1–2), 5–31.

Vicente-Serrano, S. M., Beguería, S., & López-Moreno, J. I. (2010). A Multiscalar Drought Index Sensitive to Global Warming: The Standardized Precipitation Evapotranspiration Index. *Journal of Climate*, *23*(7), 1696–1718.

Vittecoq, B., Lachassagne, P., Lanini, S., & Maréchal, J. C. (2010). Évaluation des ressources en eau de la Martinique: Calcul spatialisé de la pluie efficace et validation à l'échelle du bassin versant. *Revue Des Sciences de l'eau*, *23*(4), 361–373.

Wada, Y., Van Beek, L. P. H., Wanders, N., & Bierkens, M. F. P. (2013). Human water consumption intensifies hydrological drought worldwide. *Environmental Research Letters*, *8*(3), 034036.

Xu, Y., Gao, X., & Giorgi, F. (2010). Upgrades to the reliability ensemble averaging method for producing probabilistic climate-change projections. *Climate Research*, *41*, 61–81.

Yang, T., Ding, J., Liu, D., Wang, X., & Wang, T. (2019). Combined Use of Multiple Drought Indices for Global Assessment of Dry Gets Drier and Wet Gets Wetter Paradigm. *Journal of Climate*, *32*(3), 737–748.

Zeybekoğlu, U., & Aktürk, G. (2021). A comparison of the China-Z Index (CZI) and the Standardized Precipitation Index (SPI) for drought assessment in the Hirfanli Dam basin in central Turkey. *Arabian Journal of Geosciences*, *14*(24), 2731.

Zhao, Y. (2015). *Investigation of uncertainties in assessing climate change impacts on the* *hydrology of a Canadian river watershed* [Phd, École de technologie supérieure].